Density-functional global optimization of gold nanoclusters

Edoardo Aprà,[1] Riccardo Ferrando,[2] and Alessandro Fortunelli[3,*]
[1]*William R. Wiley Environmental Molecular Sciences Laboratory, Pacific Northwest National Laboratory, Richland, Washington 99352, USA*
[2]*Dipartimento di Fisica dell'Università di Genova, Via Dodecaneso 33, Genova, I16146, Italy*
[3]*Molecular Modeling Laboratory, IPCF-CNR, Via G. Moruzzi 1, Pisa, I56124, Italy*
(Received 27 January 2006; revised manuscript received 30 March 2006; published 18 May 2006)

The structure of gas-phase gold clusters of size ~20 is studied by density-functional global optimization in the full configuration space. The putative global minimum of Au_{20} is confirmed to be a tetrahedron (T_d) independently of the choice of the exchange-correlation functional, whereas the structure of the low-lying excited states depends on the theoretical approach. The peculiar stability of T_d is rationalized in terms of the synergic effects of *s-d* hybridization and electronic shell closure. Calculations on Au_{16} and Au_{18} show that T_d Au_{20} possibly represents a "unicum" in the sequence of gold clusters.

DOI: 10.1103/PhysRevB.73.205414 PACS number(s): 61.46.Bc, 36.40.Mr, 73.22.−f

I. INTRODUCTION

The properties of metal clusters have attracted much attention in recent years (see for example, Ref. 1) for their interesting properties and potential applications in nanotechnology. In this context, an important role is expected to be played by "magic" clusters, i.e., those possessing peculiar stability due to structural and/or electronic shell closure, whose formation energy thus exhibits a pronounced concave "cusp" as a function of size or composition, which favors preferential accumulation during growth and confers them unusual properties. Gold-based clusters are promising candidates in the search for magic structures. Gold itself occupies a unique position at the borderline between transition and simple metals, at the same time exhibiting a very large relativistic effect[2] which brings the 6*s* orbital to overlap significantly with the 5*d* orbital. Even though bulk gold is the noblest of all metals,[3] a rich and often unexpected behavior shows up in gold nanoclusters,[4] ranging from selective low-temperature catalysis of industrially important reactions, to interesting optical and electrical properties, to applications in biosensors and drug delivery thanks to its full biocompatibility. Great interest has thus arosen in connection with the discovery and characterization through photoelectron spectroscopy of the gas-phase Au_{20} cluster,[5] exhibiting an unusually large highest occupied molecular orbital (HOMO)-lowest unoccupied molecular orbital (LUMO) gap: 1.77, 0.2 eV greater than in C_{60}. On the basis of the large gap and of first-principles calculations on few selected structures, a highly symmetric tetrahedral (T_d) configuration was hypothesized [see Fig. 1(f)]. This configuration represents a piece of the fcc bulk, it is a surface-only or "cage" structure (there are no inner atoms), and its surface exhibits only fcc (111) faces. The result was puzzling from a theoretical point of view, as no existing empirical potential predicts the T_d structure as the energy minimum.[1,6] Since then, a few first-principles calculations on selected structures of Au_{20} have appeared,[7–10] confirming that T_d is more stable than several plausible competitors. However, an unbiased search of the Au_{20} global minimum has not been attempted, and the definitive assignment of the Au_{20} structure still represents an open problem.

In this paper, we perform unbiased global optimization of Au clusters in the full configuration space within a density-functional basin-hopping (DF-BH) approach. We demonstrate that the T_d structure is indeed the putative global minimum of Au_{20}, irrespectively of the choice of the exchange-correlation functional, and perform a thorough analysis of the low-lying excited states, whose ordering, on the other hand, depends on the functional. Moreover, we discover putative global minima for Au_{18} and Au_{16}, which do not belong to the T_d structural motif.

II. RESULTS AND DISCUSSION

The difficulty in locating the global minima of (metal) clusters lies in the fact that commonly employed techniques such as simulated annealing[11] are very often not exhaustive, and one has to resort to global-optimization approaches. Among these the BH algorithm[12,13] has proved to be one of the most efficient and cost effective. In the BH algorithm, the potential energy hypersurface is deformed such that to every point in the catchment basin of each local minimum the energy of that minimum is assigned. The Monte Carlo search moves then allow the system to hop from one catchment basin to another.

A first-principles description of the energetics is necessary in our case since empirical potentials are apparently not able to correctly describe the energetics of small Au clusters. Our DF calculations utilizes the Becke[14] functional for exchange and the Lee-Yang-Parr[15] functional for correlation, within the NWChem[16] suite of programs.[17]

In the case of Au_{20}, three DF-BH runs have been performed, each comprising 300 Monte Carlo steps, starting from randomly chosen initial configurations.[18] The choice of 300 Monte Carlo steps is justified by considering that BH searches conducted on Au_{20} using several different atom-atom potentials always found the corresponding global minimum within the first 300 Monte Carlo steps. In addition, the 100 lowest-energy structures obtained through an extensive BH search using an empirical potential[19] have also been locally optimized. In all three DF-BH runs, the search singled out T_d as the lowest-energy structure, locating it after 233,

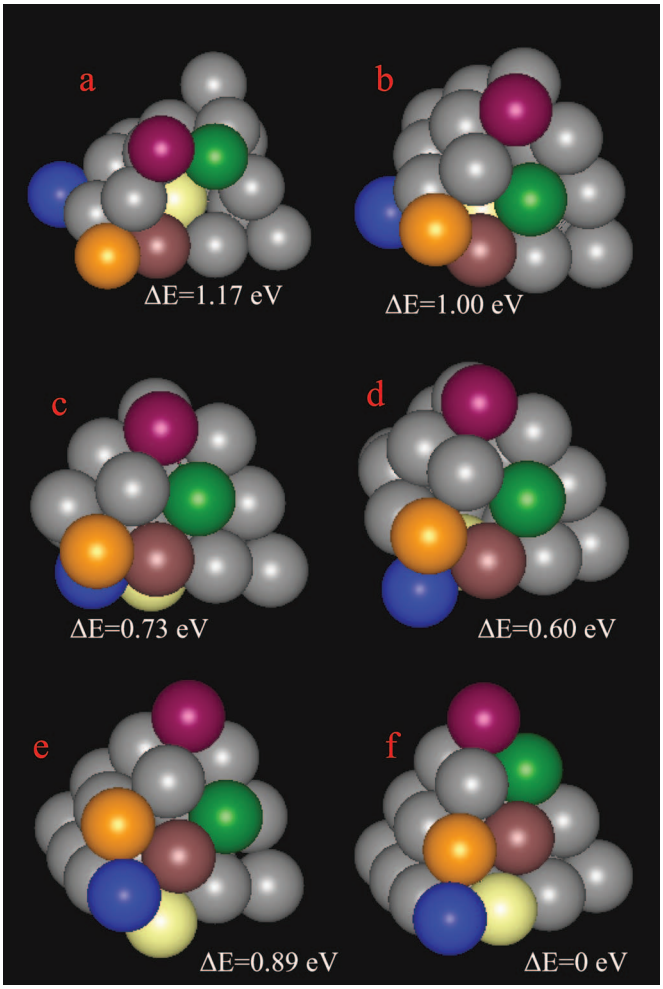

FIG. 1. (Color) Schematic pictures of selected local minima [(a)–(e)] and the T_d putative global minimum (f) from one particular DF-BH run (see text for details). ΔE represents the energy difference with respect to T_d in electron-volts (eV), according to the Becke-Lee-Yang-Parr *xc* functional.

28, and 177 steps, respectively.[20] The T_d minimum, apart from being the lowest-energy structure found by the DF-BH algorithm, also seems to have a rather large catchment basin, as proved by the fact that (1) it has been located as the putative global minimum in all the three DF-BH runs, and (2) after the algorithm locates the T_d structure, it takes 15–20 Monte Carlo steps before being able to escape from it: This is due to the large energy separation with respect to the first excited state, but also to the fact that in some of these steps the geometry optimization falls back into the T_d minimum after the random move.

Even though the BH random moves cannot be associated with real physical processes (the kinetics of the cluster reorganization), it is suggestive to interpret them as some kind of Monte Carlo jumps between basins of attraction. We thus show in Fig. 1 five configurations chosen among those 14 immediately preceding the location of the T_d putative global minimum in the third DF-BH run. These configurations have been chosen because they are highly representative examples of the low-lying excited states we encountered in our DF-BH searches, i.e., mainly cage structures, among which a substantial number of variously defective T_d. Different colors have been used to distinguish individual atoms, and allow one to follow their movements. The energy differences with respect to T_d are also shown. Figure 1(a) is a typical example of the "cage" structures that occur so frequently in our BH search: it has a relatively high energy (1.17 eV), but it is structurally not too far from a T_d. Indeed, after a BH step, it rearranges into a defective T_d [Fig. 1(b)] in which one apex atom (the blue colored one) has moved onto an edge of the tetrahedron. This is the simplest type of T_d defect, but also has a relatively high energy (1.0 eV). In the next step [Fig. 1(c)], the blue atom has inserted into the bottom fcc (111) face, giving another common type of a defective T_d. A further rearrangements [Fig. 1(d)] brings this atom onto the vertex of a triangular pyramid whose three basal atom lye in a corner of the bottom fcc (111) face. This configuration can also be described as a defective T_d, and, according to our calculations, it corresponds to the lowest-energy isomer above the T_d putative global minimum. From here, through an intermediate configuration slightly higher in energy [Fig. 1(e)], in which the blue atom has moved to an apex position, dragging the atom at the center of the fcc (111) face onto an edge of the tetrahedron, a configuration which is thus intermediate between a generic cage structure and a defective T_d, the T_d putative global minimum is finally attained [Fig. 1(f)]. It can be noted that the HOMO-LUMO gap of T_d Au_{20} is 1.96 eV, in agreement with previous calculations, but the defective T_d first excited state [Fig. 1(d)] also has a significant gap (1.49 eV).

Other low-lying excited states found in our DF-BH searches and different from those shown in Fig. 1 are reported in Fig. 2: They correspond to other defective T_d [Figs. 2(a) and 2(b)], doubly defective T_d [Figs. 2(c) and 2(d)], and a cage structure [Fig. 2(e)]. The most stable compact configuration [Fig. 2(f)] obtained via local minimization of the 100 lowest-energy structures obtained using an empirical potential[19] is also shown. It can be noted that Fig. 2(a) is taken from the second DF-BH run, Fig. 2(b) from the third, Fig. 2(c) from the first DF-BH run, Fig. 2(d) from the second DF-BH run, Fig. 2(e) from the third DF-BH run: This shows that there is a qualitative overlap among the three DF-BH runs. To give an idea of the statistics of our DF-BH searches, a histogram showing the cumulative energy distribution of the structures found in our BH searches is shown in Fig. 3: From this figure, it is apparent that the energy range beyond $\approx$1.7 eV above the T_d putative global minimum is more and more poorly sampled with increasing ΔE.

No compact, space-filled configurations could be located within 1 eV of the T_d putative global minimum: The most stable isomer obtained from the local geometry optimization of the empirical potential[19] structures [see Fig. 2(f)] lies at 1.28 eV. In contrast, a planar structure [a Au_{21} triangle cut out of an fcc (111) face and missing one apex atom] lies only slightly above the T_d-defected first excited state [Fig. 1(d)]: This is not surprising, as planar structures are the global minima of slightly smaller gold clusters and anions.[21,22] This explains why it is so difficult to find the T_d minimum via unbiased combined empirical potential/DF searches: At the

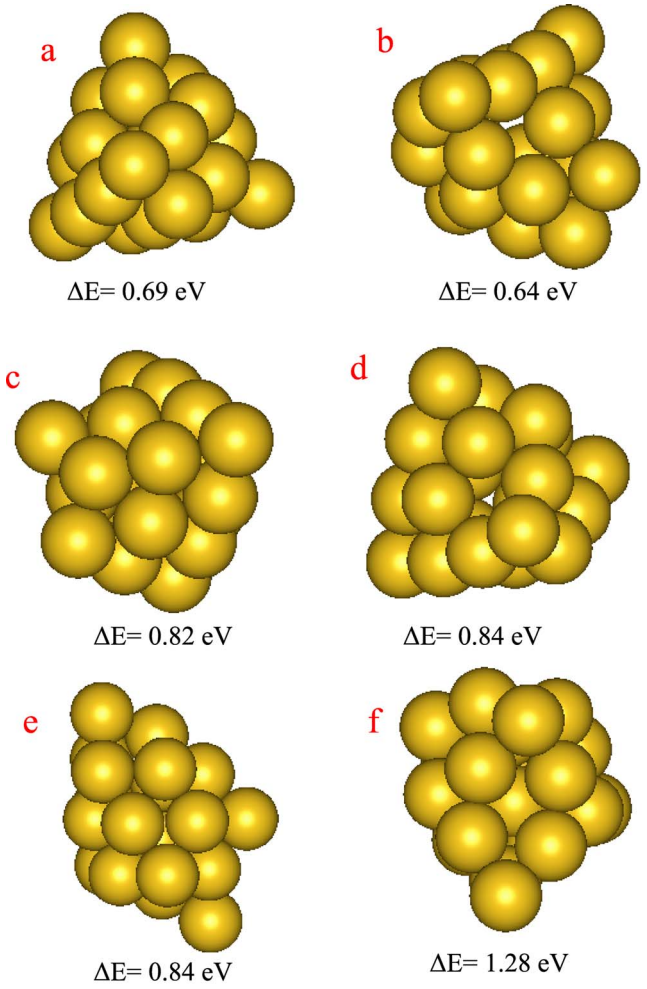

FIG. 2. (Color online) Schematic pictures of a few low-lying excited states from our BH searches different from those shown in Fig. 1: defective T_d [(a), (b)], doubly defective T_d [(c), (d)], and a cage structure (e). The most stable compact configuration (f) obtained via local minimization of the 100 lowest-energy structures obtained using an empirical potential (see Ref. 19) is also shown. ΔE represents the energy difference with respect to T_d in eV, according to the Becke-Lee-Yang-Parr *xc* functional.

empirical potential[19] level, T_d lies at 1.08 eV above the global minimum, and is estimated to be the 1300th excited state. Also biased empirical potential/DF searches often miss to predict the true lowest-energy structure. As an example, the defective T_d structures predicted by a biased combined empirical potential/DF search as global minima for Au_{18} and Au_{16} (Ref. 10) (i.e., Au_{20} tetrahedra missing two or four apex atoms, respectively) are not the lowest-energy structures according to our calculations. By performing a few tens of DF-BH steps using the same *xc* functional[23] as in Ref. 10 we could easily find several isotops, structurally different from the global minima proposed in Ref. 10, but either nearly degenerate with them (for Au_{18}) or more stable by $\geqslant$0.5 eV (for Au_{16}). In Fig. 4, the defective T_d missing four apex atoms proposed as global minimum in Ref. 10 and a low-symmetry cluster from our DF-BH search lying below the former by 0.71 eV are shown for Au_{16}. It can thus be

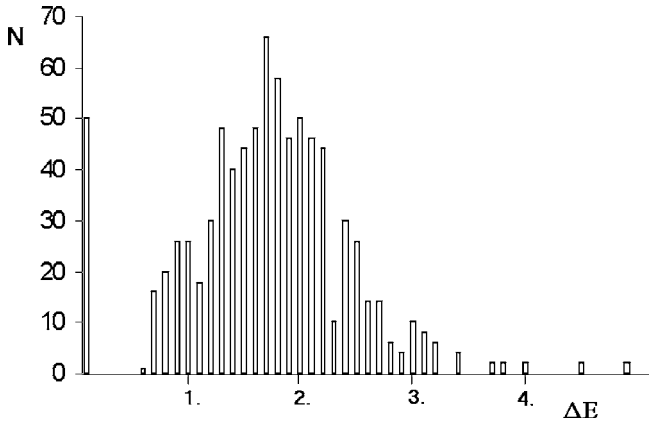

FIG. 3. Histogram showing the cumulative energy distribution of the structures found in our BH searches. The first peak contains the T_d putative global minimum. ΔE in eV.

concluded that only an unbiased, fully first-principles global-optimization approach like the one employed in the present work does furnish a reasonable guarantee that the true DF global minimum is located, at the same time providing with a set of candidates for the low-lying excited states.

The peculiar stability of the T_d can be rationalized in terms of three main reasons: (1) stickiness of the Au-Au bonding; (2) directionality effects in the Au-Au interaction; and (3) electronic shell closure.

Stickiness of the Au-Au bonding. The limited spatial extension of the Au 6*s* orbital (due to the relativistic contraction) translates into a shorter-range atom-atom interaction as compared to first-row and second-row transition metals, and thus to a high energetic penalty for changing the interatomic distances from their optimal (coordination-dependent) value.[24] This disfavors icosahedral configurations, which are competitive in this size range in terms of bond counting but present a large internal strain, and favors possibly amorphous or—for very small clusters such as Au_{20}—surface-only or cage structures, such as the T_d.

Directionality effects. The relativistic contraction of the *s* orbital brings it to substantially overlap with the *d* orbitals, decreasing the localized character of the latter and strongly increasing their contribution to chemical bonding. This in turn implies a substantial anisotropy of the Au-Au bonding: Not only the number, but also the spatial arrangement of the neighbors matters in terms of binding energy. For gold, in

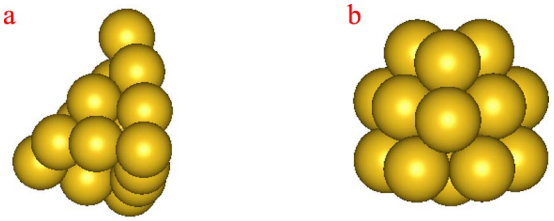

FIG. 4. (Color online) Schematic pictures of the Au_{16} defective T_d (b) and a structurally different configuration (a) lower in energy by 0.71 eV according to the PW91 *xc* functional (see Ref. 23) used in Ref. 10.

particular, this disfavors asymmetric arrangements. For example, a fcc (111) bilayer (coordination number=9, but strongly asymmetric bonding environment) has a binding energy per atom only 0.08 eV greater than that of a single fcc (111) monolayer (coordination number=6, but symmetric bonding environment). In other words, there is a small energy penalty in dissociating a fcc (111) bilayer into two fcc (111) monolayers, and this again favors surface-only or cage structures with low-coordinated atoms arranged according to local fcc patterns (see Ref. 25 for a more detailed discussion).

Electronic shell closure. $N=20$ and $N=18$ correspond to electronic magic numbers for various different models. For $N=20$: spherical electron gas,[26] tetrahedral electron gas.[27] For $N=18$: tensor surface harmonic Theory;[28] hard-well layered electron gas;[29] Hirsch $2(N+1)^2$ rule for spherical aromaticity.[30] It is thus not surprising to encounter clusters exhibiting large HOMO-LUMO gaps in this size range. This means that a large HOMO-LUMO gap does *not* automatically implies that the cluster is of high symmetry: As it happens, the information derived from electron spectroscopy measurements does not provide *per se* a complete structural characterization. The scheme of the one-electron energy levels of T_d indeed conforms to that predicted by jellium models.[4] However, here again the *s-d* interaction plays a significant role. First, by performing a *s-d* decomposition of the DF wave function[31] we found an appreciable *s-d* orbital mixing. Moreover, to provide a clearer evidence, we implemented an approach[32] in which the Au atom is described as a one-electron element, i.e., in which the *d* orbitals are separated from the *s* orbitals and included into the core, and we performed a DF-BH run. After a few tens of steps starting from the T_d configuration, the system evolved into low-symmetry compact, space-filled structures qualitatively similar to those predicted as global minimum or low-lying excited states by the empirical potential,[19] and more stable than T_d by 0.5–1.0 eV. It is interesting to note that in this approach the T_d HOMO-LUMO gap is 2.63 eV, i.e., even greater than that predicted by the all-electron approach, but that of several low-symmetry low-energy structures is also large: About 1.8 eV. This explains why T_d is not the global minimum of Cu_{20}, Ag_{20}, etc.[7,9] At the one-electron level, in the absence of *s-d* hybridization, the extra stability assured by tetrahedral aromaticity[27] is counteracted by other structural factors, such as the preference for compact arrangements (which are also favored by spherical aromaticity at $N=20$). In contrast, for T_d Au_{20} the stability induced by tetrahedral aromaticity (which can be quantified in 0.5–1.0 eV) is reinforced by the tendency of small gold clusters towards open, cage configurations, a tendency ultimately relying on *s-d* hybridization. As noted above, this is no more true for $N\neq 20$, so that T_d structures missing apex atoms are not the global minima for Au_{16} and Au_{18}. The T_d structure of Au_{20} thus possibly represents a "unicum" in the structural sequence of gold clusters.[9]

Finally, it has been observed that DF predictions of the structure of gold clusters are affected (sometimes appreciably) by the choice of the *xc* functional, the effective core potential and the numerical approach.[8,9,32] Under this respect, we found the Au_{20} T_d structure to be remarkably stable under a variety of DF approaches. We performed in fact further DF-BH test runs and properly selected local geometry optimizations using the local density approximation or a different *xc* functional,[23] employing more extended Gaussian-type orbital or plane wave basis sets, and we always found that T_d remains the ground state. Selected results from these calculations are reported in Table I. From this table, it can be seen that what changes when changing the *xc* functional is the nature of the lowest-energy excited states, switching from open (cage) arrangements for the Becke-Lee-Yang-Parr functionals, to compact, space-filled configurations (similar to those reported in Ref. 8) for the local density approximation. A more detailed study will be reported in the future.[25]

TABLE I. Relative energies of various structures of Au_{20} clusters from DF calculations. T_d is the putative tetrahedral global minimum [Fig. 1(f)], defective-T_d corresponds to Fig. 1(d), compact corresponds to Fig. 2(f). BLYP is the Becke-Lee-Yang-Parr *xc* functional, PW91 the Perdew-Wang *xc* functional (see Ref. 23), LDA is the local density approximation. GTO means Gaussian-type-orbitals (see Ref. 38), PW means plane waves (see Ref. 39).

Cluster	BLYP/GTO	PW91/GTO	PW91/PW	LDA/PW
T_d	0.00	0.00	0.00	0.00
Defective T_d	0.60	0.88	0.89	0.96
Compact	1.26	1.30	1.33	0.77

III. CONCLUSIONS

We have implemented a DF-BH approach, and applied it to the determination of the global minimum and low-energy excited state structures of gas-phase Au_{20}. Three DF-BH runs are conducted, each comprising 300 DF-BH steps, plus additional local geometry optimizations starting from the 100 lowest-energy structures according to an empirical potential. The putative global minimum of Au_{20} is confirmed to be a T_d, independently of the choice of *xc*-functional or the numerical approach, whereas the structure of low-lying excited states depends on the theoretical approach, switching from open (cage)—such as defective T_d—arrangements, to compact, space-filled configurations. The peculiar stability of T_d is rationalized in terms of the synergic effects of *s-d* hybridization, which makes the Au-Au interaction very sticky and directional, thus favoring open structures exhibiting local fcc patterns, and electronic shell closure, associated with tetrahedral aromaticity. Calculations on Au_{16} and Au_{18} using two different gradient-corrected *xc* funxtionals show that low-symmetry arrangements structurally different from defective T_d are either competitive or at an appreciably lower energy, suggesting that T_d Au_{20} possibly represents a unicum in the structural sequence of gold clusters.

ACKNOWLEDGMENTS

We acknowledge financial support from the Italian CNR for the project "(Supra-)Self-Assemblies of Transition Metal Nanoclusters" within the framework of the ESF EURO-

CORES SONS, and from European Community Sixth Framework Programme for the project "Growth and Supra-Organization of Transition and Noble Metal Nanoclusters" (Contract No. NMP4-CT-2004-001594). A portion of the research described in this manuscript was performed at the W.R. Wiley EMSL, a national scientific user facility sponsored by the U.S. DOE OBER and located at PNNL. PNNL is operated for the DOE by Battelle.

*Author to whom correspondence should be addressed; email address: fortunelli@ipcf.cnr.it

[1] F. Baletto and R. Ferrando, Rev. Mod. Phys. **77**, 371 (2005).
[2] P. Pyykkö, Angew. Chem., Int. Ed. **43**, 4412 (2004).
[3] B. Hammer and J. K. Norskov, Nature (London) **376**, 238 (1995).
[4] M.-C. Daniel and D. Astruc, Chem. Rev. (Washington, D.C.) **104**, 293 (2004).
[5] J. Li, X. Li, H.-J. Zhai, and L.-S. Wang, Science **299**, 864 (2003).
[6] N. T. Wilson and R. L. Johnston, Eur. Phys. J. D **12**, 161 (2000).
[7] J. Wang, G. Wang, and J. Zhao, Chem. Phys. Lett. **380**, 716 (2003).
[8] B. Soulé de Bas, M. J. Ford and M. B. Cortie, J. Mol. Struct.: THEOCHEM **686**, 193 (2004).
[9] E. M. Fernández, J. M. Soler, I. L. Garzón, and L. C. Balbás, Phys. Rev. B **70**, 165403 (2004).
[10] W. Fa, C. Luo, and J. Dong, Phys. Rev. B **72**, 205428 (2005).
[11] S. Kirkpatrick, C. D. Gelatt, Jr., and M. P. Vecchi, Science **270**, 671 (1983).
[12] Z. Li and H. A. Scheraga, Proc. Natl. Acad. Sci. U.S.A. **84**, 6611 (1987).
[13] D. J. Wales and J. P. K. Doye, J. Phys. Chem. A **101**, 5111 (1997).
[14] A. D. Becke, Phys. Rev. A **38**, 3098 (1988).
[15] C. Lee, W. Yang, and R. G. Parr, Phys. Rev. B **37**, 785 (1988).
[16] E. Aprà *et al.*, NWCHEM, A Computational Chemistry Package for Parallel Computers, Version 4.7, 2005, Pacific Northwest National Laboratory, Richland, WA 99352-0999.
[17] We use a $(7s,5p,5d)/[6s,3p,2d]$ Gaussian-type-orbital basis set (see Ref. 33), a scalar-relativistic effective-core potential (see Ref. 34), an auxiliary $(9s,4p,4d,3f,4g)/[8s,4p,3d,3f,2g]$ basis set (see Refs. 35 and 36) for the expansion of the electron density, a numerical grid of 65 radial points and 350 Lebedev angular points for evaluating the *xc* potential and energy, and a smearing factor of 0.005 a.u., see Ref. 37 for more details on the numerical procedure. All the calculations are spin unrestricted. The geometry optimizations were stopped after a threshold of 0.004 a.u./Å on the gradient and 0.019 Å on the difference in Cartesian coordinates of the atoms was reached.
[18] The initial states have been generated by randomly distributing the atoms in a sphere of 6 Å radius. A random move of up to 1 Å (positive or negative) in the Cartesian coordinates of each atom was allowed. A value of 0.5 eV was chosen as kT in the Monte Carlo check.
[19] V. Rosato, M. Guillopé, and B. Legrand, Philos. Mag. A **59**, 321 (1989). The following parameters have been used: $A=0.2197$ eV, $\xi=1.855$ eV, $p=10.53$, $q=4.3$, $r_0=2.885$ Å.
[20] The NWCHEM self-consistent algorithm proved to be rather robust, always converging in all the 1000 geometry optimizations we conducted. On average, the first scf process reached convergence in about 30–37 iterative steps in 90% of the cases (never exceeding 54 iterative steps in the remaining 10% cases), and typically in about ten iterative steps for the successive iterative processes. Note that our random moves do not exceed 1 Å in absolute value in each coordinate, which implies that the random configurations generated in the Monte Carlo steps usually do not have too small internuclear distances.
[21] H. Häkkinen, M. Moseler, and U. Landman, Phys. Rev. Lett. **89**, 033401 (2002).
[22] F. Furche, R. Ahlrichs, P. Weis, C. Jacob, S. Gilb, T. Bierweiler, and M. M. Kappes, J. Chem. Phys. **117**, 6982 (2002).
[23] J. P. Perdew, J. A. Chevary, S. H. Vosko, K. A. Jackson, M. R. Pederson, D. J. Singh, and C. Fiolhais, Phys. Rev. B **46**, 6671 (1992).
[24] J. P. K. Doye, D. J. Wales, and R. S. Berry, J. Chem. Phys. **103**, 251 (2000).
[25] S. Olivier and G. Barcaro, A. Fortunelli (unpublished).
[26] M. Brack, Rev. Mod. Phys. **65**, 677 (1993).
[27] S. M. Reimann, M. Koskinen, H. Häkkinen, P. E. Lindelof, M. Manninen, and Phys. Rev. B **56**, 12147 (1997).
[28] A. J. Stone, Inorg. Chem. **20**, 563 (1981).
[29] R. Ferrando, A. Fortunelli, and G. Rossi, Phys. Rev. B **72**, 085449 (2005).
[30] A. Hirsch, Z. Chen, and H. Jiao, Angew. Chem., Int. Ed. **39**, 3915 (2000).
[31] A. Fortunelli and A. M. Velasco, Int. J. Quantum Chem. **97**, 654 (2004).
[32] V. Bonačič-Koutecky, J. Burda, R. Mitrič, M. Ge, G. Zampella, and P. Fantucci, J. Chem. Phys. **117**, 3120 (2002).
[33] D. Andrae, U. Haeussermann, M. Dolg, H. Stoll, and H. Preuss, Theor. Chim. Acta **77**, 123 (1990).
[34] M. Dolg, U. Wedig, H. Stoll, and H. Preuss, J. Chem. Phys. **86**, 866 (1987).
[35] A. Fortunelli and O. Salvetti, J. Comput. Chem. **12**, 36 (1991).
[36] K. Eichkorn, O. Treutler, H. Öhm, M. Häser, and R. Ahlrichs, Chem. Phys. Lett. **240**, 283 (1995).
[37] E. Aprà and A. Fortunelli, J. Phys. Chem. **107**, 2934 (2003).
[38] The Kohn-Sham equations are solved on a large $(9s,8p,6d,3f,1g)/[7s,5p,4d,3f,1g]$ basis set of Gaussian-type-orbitals (see Ref. 33) using an auxiliary $(9s,4p,5d,4f,5g,3h)/[8s,4p,4d,4f,5g,3h]$ basis set (see Ref. 36) for the expansion of the electron density and a scalar-relativistic effective-core potential (see Ref. 34).
[39] The DF calculations are performed using the plane-wave self-consistent field (PWSCF) computational code (see Ref. 40), employing a plane-wave basis set, ultrasoft pseudopotentials, a kinetic energy cutoff for the selection of the plane-wave basis set of 40 Ry (1 Ry=13.6 eV), and the Gamma point for the *k*-point sampling of the Brillouin zone. The dimension of the unit cell is chosen so as to leave a distance of 6–8 Å between atoms on neighboring cell images.
[40] S. Baroni, A. Del Corso, S. de Gironcoli, and P. Giannozzi, http://www.pwscf.org